Proton Transfer Reactions in the F86D and F86E Mutants of *pharaonis* Phoborhodopsin (Sensory Rhodopsin II)†

Masayuki Iwamoto,‡ Yuji Furutani,§,||,⊥ Naoki Kamo,‡ and Hideki Kandori*,§,⊥

Laboratory of Biophysical Chemistry, Graduate School of Pharmaceutical Sciences, Hokkaido University, Sapporo 060-0812, Japan, Department of Applied Chemistry, Nagoya Institute of Technology, Showa-ku, Nagoya 466-8555, Japan, Department of Biophysics, Graduate School of Science, Kyoto University, Sakyo-ku, Kyoto 606-8502, Japan, and Core Research for Evolution Science and Technology (CREST), Japan Science and Technology Corporation, Kyoto 606-8502, Japan

Received October 17, 2002; Revised Manuscript Received January 19, 2003

ABSTRACT: *pharaonis* phoborhodopsin (*p*pR, also called *pharaonis* sensory rhodopsin II, *p*sRII), a negative phototaxis receptor of *Natronobacterium pharaonis*, can use light to pump a proton in the absence of its transducer protein. However, the pump activity is much lower than that of the light-driven proton-pump bacteriorhodopsin (BR). *p*pR's pump activity is known to be increased in a mutant protein, in which Phe86 is replaced with Asp (F86D). Phe86 is the amino acid residue corresponding to Asp96 in BR, and we expect that Asp86 plays an important role in the proton transfer at the highly hydrophobic cytoplasmic domain of the F86D mutant *p*pR. In this article, we studied protein structural changes and proton transfer reactions during the photocycles of the F86D and F86E mutants in *p*pR by means of Fourier transform infrared (FTIR) spectroscopy and photoelectrochemical measurements using a tin oxide (SnO_2) electrode. FTIR spectra of the unphotolyzed state and the K and M intermediates are very similar among F86D, F86E, and the wild type. Asp86 or Glu86 is protonated in F86D or F86E, respectively, and the pK_a > 9. During the photocycle, the pK_a is lowered and deprotonation of Asp86 or Glu86 is observed. Detection of both deprotonation of Asp86 or Glu86 and concomitant reprotonation of the 13-*cis* chromophore implies the presence of a proton channel between position 86 and the Schiff base. However, the photoelectrochemical measurements revealed proton release presumably from Asp86 or Glu86 to the cytoplasmic aqueous phase in the M state. This indicates that the *p*pR mutants do not have the BR-like mechanism that conducts a proton uniquely from Asp86 or Glu86 (Asp96 in BR) to the Schiff base, which is possible in BR by stepwise protein structural changes at the cytoplasmic side. In *p*pR, there is a single open structure at the cytoplasmic side (the M-like structure), which is shown by the lack of the N-like protein structure even in F86D and F86E at alkaline pH. Therefore, it is likely that a proton can be conducted in either direction, the Schiff base or the bulk, in the open M-like structure of F86D and F86E.

pharaonis phoborhodopsin (*p*pR,[1] also called *pharaonis* sensory rhodopsin II, *p*sRII) (*1*−*8*) is a member of an archaeal rhodopsin family and acts as a negative phototaxis receptor for *Natronobacterium pharaonis*. The phototaxis is achieved by modulating the cell swimming behavior through light-activated signal transduction from *p*pR to its cognate transducer protein, *p*HtrII. *p*pR has seven transmembrane helices, on one of which the chromophore, all-*trans*-retinal, binds through a protonated Schiff base. This feature is common among other archaeal rhodopsins such as bacteriorhodopsin (BR) (*9*, *10*), halorhodopsin (HR) (*11*−*13*), and sensory rhodopsin (sR or sRI) (*14*−*16*) which are an outwardly light-driven proton pump, an inwardly light-driven Cl pump, and another sensor of phototaxis, respectively. Many investigations concerning the structure and function of BR have been reported, and consequently, BR is one of the best understood membrane proteins at present. On the other hand, the other archaeal rhodopsins are less well understood.

Functional expression of *p*pR in *Escherichia coli* cells has been achieved (*17*), which affords a large amount of protein to be characterized in detail (see ref *18* for review). The crystal structure of *p*pR was determined in 2001 by two groups (*19*, *20*). Very recently, the crystal structure of the *p*pR−*p*HtrII complex has been reported (*21*). These advances opened the next stage of research on this photosensor.

The photocycle intermediates in *p*pR have been denoted K−O in analogy to those in BR. Nevertheless, there are certain differences in their photocycles between *p*pR and BR.

† This work was supported by grants from the Japanese Ministry of Education, Culture, Sports, Science, and Technology to H.K. and by Research Fellowships from the Japan Society for the Promotion of Science for Young Scientists to M.I.

* To whom correspondence should be addressed. Phone and Fax: 81-52-735-5207. E-mail: kandori@ach.nitech.ac.jp.

‡ Hokkaido University.

§ Nagoya Institute of Technology.

|| Kyoto University.

⊥ Japan Science and Technology Corp.

[1] Abbreviations: *p*pR, *pharaonis* phoborhodopsin; *p*pR_K, K intermediate of *p*pR; *p*pR_M, M intermediate of *p*pR; *p*pR_O, O intermediate of *p*pR; BR, light-adapted bacteriorhodopsin that has all-*trans*-retinal as its chromophore; BR_M, M intermediate of BR; BR_N, N intermediate of BR; FTIR, Fourier transform infrared; DM, *n*-dodecyl *β*-D-maltoside; PC, L-α-phosphatidylcholine.

10.1021/bi0270283 CCC: $25.00
Published on Web 02/15/2003

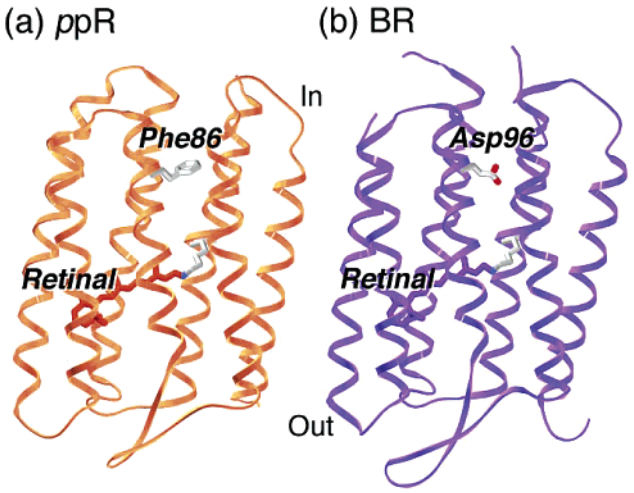

FIGURE 1: X-ray crystallographic structures of *p*pR (a) and BR (b). The retinal chromophore, which is bound to Lys205 or Lys216 on helix G through the Schiff base, and Phe86 or Asp96 are depicted as bold sticks in the ribbon drawing of the backbone structures of *p*pR and BR, respectively. These structures were taken from the Protein Data Bank [entry 1H68 for *p*pR (*20*) and entry 1C3W for BR (*54*)].

The K intermediate is highly stable in *p*pR, and the L intermediate of *p*pR can be observed only at room temperature (*22*, *23*). The presence of the N intermediate was suggested by multiexponential global analysis of the photocycle of *p*pR (*1*), but it is not well-understood. In fact, one FTIR study of ours revealed that *p*pR does not possess an N-like protein structure that is characteristic of the N intermediate of BR (*24*). *p*pR can pump protons from the cytoplasmic to the extracellular side in the absence of a transducer (*25*−*27*), but the pump efficiency is low (*26*).

One of the remarkable differences is that *p*pR lacks an internal proton donor for reprotonation of the Schiff base via a cytoplasmic proton-conducting channel. In BR, Asp96 donates a proton to the Schiff base from the cytoplasmic side in the M-to-N transition. The corresponding amino acid residue in *p*pR is Phe86 (Figure 1). Therefore, in the proton pump of *p*pR, a proton must be transferred from an aqueous phase to the deprotonated Schiff base in the decay of the M intermediate. It was reported that replacement of Phe86 with Asp (F86D) increases the proton pumping activity of *p*pR (*25*), suggesting that Asp86 can act as an internal proton donor, like Asp96 in BR. Is the replacement of a single amino acid at position 86 sufficient to convert *p*pR into a BR-like pump? It is noted that the photocycle kinetics of F86D are similar to those of wild-type *p*pR, both being much longer than those of BR (*25*, *28*).

In this paper, we analyzed proton transfer reactions during the photocycles of F86D and F86E (Phe86 to Glu) in *p*pR by using Fourier transform infrared (FTIR) spectroscopy and photocurrent measurements. FTIR spectroscopy is a powerful tool for studying the molecular structure and structural changes of rhodopsins. It is particularly useful in investigating protonation changes in carboxylates, and the correlation with changes in retinal chromophore and protein structures. Using this method, light-induced structural changes in F86D and F86E were compared with those of the wild type with regard to the K (*22*) and M (*24*) intermediates. In addition, photoelectrochemical measurements using a SnO_2 electrode (*29*−*37*) were applied in investigating transient pH changes during the photocycles. Low-temperature FTIR spectroscopy clearly showed that Asp86 and Glu86 are protonated in F86D and F86E, respectively, and transiently deprotonated during the photocycle. Concomitant protonation of the retinal Schiff base suggests the proton transfer occurs from Asp86 or Glu86 to the Schiff base. However, photoelectrochemical measurements showed the presence of light-induced fast proton release presumably from Asp86 or Glu86 to the cytoplasmic aqueous phase. Protein structure and proton movement during the photocycle were discussed by combining the results obtained from the two different measurements.

MATERIALS AND METHODS

Preparation of the ppR Sample. Mutant proteins of *p*pR were prepared as described previously (*22*, *28*). Briefly, the *p*pR proteins possessing a histidine tag at the C-terminus were expressed in *E. coli*, solubilized with 1.5% *n*-dodecyl *β*-D-maltoside (DM), and purified with a Ni column. The purified *p*pR sample was then reconstituted into L-α-phosphatidylcholine (PC) liposome by dialysis, where the molar ratio of the added PC was 50 times that of *p*pR.

FTIR Spectroscopy. FTIR spectroscopy was applied as described previously (*22*, *24*, *38*). The *p*pR sample in PC liposomes was washed twice with buffer at pH 7.0 (2 mM phosphate) or 9.0 (2 mM borate). Ninety microliters of the *p*pR sample was dried on a BaF_2 window with a diameter of 18 mm. After hydration by either H_2O or D_2O, the sample was placed in a cell, which was mounted in an Oxford DN-1704 cryostat equipped in the Bio-Rad FTS-40 spectrometer.

The ppR_K minus *p*pR difference spectra were measured as follows (*22*). Illumination of the *p*pR film at pH 7.0 with 450 nm light at 77 K for 2 min converted *p*pR to ppR_K, and subsequent illumination with >560 nm light changed ppR_K back into *p*pR. The difference spectrum was calculated from the spectra constructed with 128 interferograms before and after the illumination. Twenty-four spectra obtained in this way were averaged for the ppR_K minus *p*pR spectrum.

The ppR_M minus *p*pR difference spectra were measured at 250 K and pH 7.0 as follows (*24*). To convert *p*pR to ppR_M, the sample was irradiated for 90 s with >480 nm light; subsequent illumination with UV light changed ppR_M back into *p*pR. The difference spectrum was calculated from the spectra constructed with 64 interferograms after minus before the illumination. Twenty-four spectra obtained in this way were averaged for the ppR_M minus *p*pR spectrum.

For the measurement of the N-like intermediate of the *p*pR mutants, we used an alkaline film (pH 9.0). The sample was illuminated with >480 nm light for 60 s at 270 K. The N-like intermediate that formed reverted to the original state within 2 min at 270 K, as shown by the similar but inverted spectral shape. The difference spectrum was calculated from the spectra constructed with 32 interferograms before and after the illumination. Twenty-four spectra obtained in this way were averaged.

Photoelectrochemical Measurements. The apparatus was essentially the same as described previously (*37*) except for the samples. The *p*pR sample reconstituted into PC liposomes was used here instead of the DM-solubilized sample used for the previous study (*37*). The *p*pR sample in PC liposomes was washed twice with distilled water. Fifty microliters of the *p*pR sample was dried on a SnO_2 electrode with a

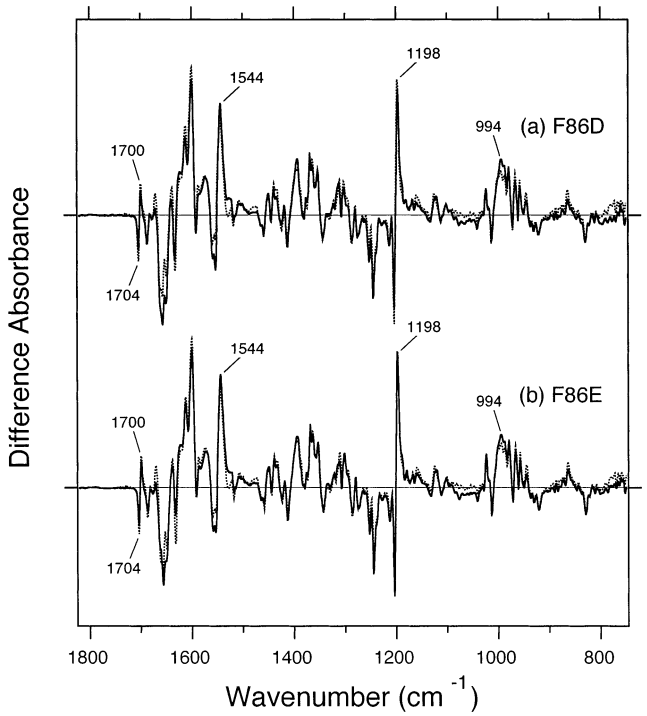

FIGURE 2: *p*pR$_K$ minus *p*pR IR difference spectra of F86D (a) and F86E (b) in the 1820−760 cm^{-1} region. Difference IR spectra of the wild type (*22*) are reproduced as dotted lines for comparison.

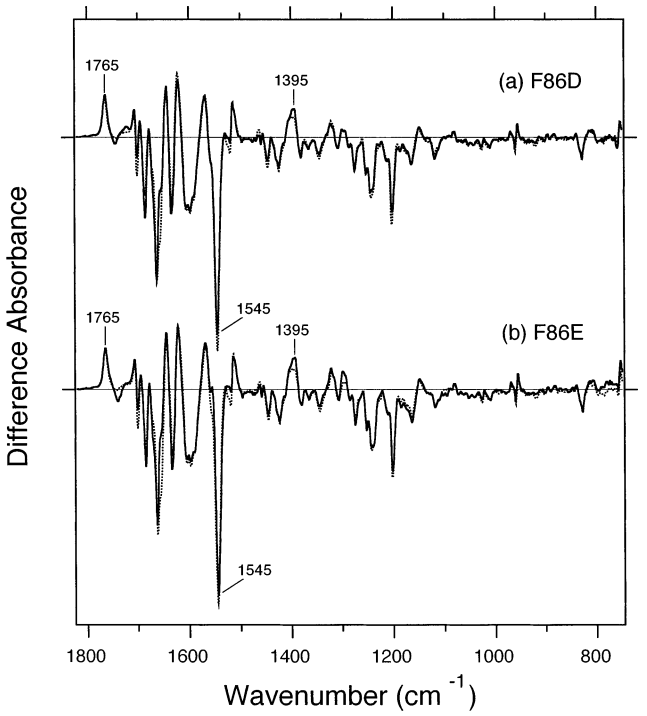

FIGURE 3: *p*pR$_M$ minus *p*pR IR difference spectra of F86D (a) and F86E (b) in the 1820−760 cm^{-1} region. Spectra are measured at 250 K and pH 7. Difference IR spectra of the wild type (*24*) are reproduced as dotted lines for comparison.

diameter of 10 mm. A pair of SnO_2 electrodes was used: one of them as a working electrode on which the sample was deposited and the other as the counter electrode. The cell was composed of SnO_2, a thin deposited *p*pR layer, an electrolyte solution, and SnO_2. The electrolyte solution contained 0.13 M Na_2SO_4 and a mixture of six buffers (citric acid, MES, HEPES, MOPS, CHES, and CAPS, whose concentrations were 1 mM each). The mixture of six buffers has almost equal buffer capacity for the whole pH range that was studied. The pH was adjusted with H_2SO_4 or NaOH to the desired value.

The light source was a 300 W xenon arc lamp in combination with an infrared cutoff filter and color filter (HA50 and Y44, Toshiba), which provided >440 nm light. The actinic light, the duration time of which was 4 ms, was provided to the electrochemical cell through a mechanical shutter. The two SnO_2 electrodes were connected to an amplifier (Bioelectric Amplifier MEG-1200, Nihon Koden) equipped with low-cut filters ranging from 0.08 to 150 Hz. The low-cut frequency was set to 15 Hz in these measurements. The output of this amplifier was connected to a digital oscilloscope (Hewlett-Packard model 54520C) to store the signal.

RESULTS

Infrared Spectral Changes of the F86D and F86E Mutants of ppR upon Formation of the K Intermediate. Figure 2 shows the *p*pR$_K$ minus *p*pR infrared difference spectra of F86D (a) and F86E (b) measured at 77 K and pH 7. The spectra are compared with the previously reported spectrum for the wild-type protein (···) (*22*). Almost identical difference spectra were obtained for F86D and F86E, indicating similar structural changes on formation of the K intermediate. The positive bands at 1544, 1198, and 994 (+) cm^{-1} correspond to the C═C stretch, C−C stretch, and hydrogen out-of-plane (HOOP) vibrations of the retinal chromophore in the K intermediate, respectively (*22*). The characteristic vibrational bands at 1704 (−) and 1700 (+) cm^{-1} have been assigned as the C═O stretching vibrations of Asn105 in *p*pR and *p*pR$_K$, respectively (*39*).

There are no spectral changes in the 1800−1710 cm^{-1} region, where protonated carboxylic C═O stretching vibrations appear. This indicates there are no structural changes of Asp86 and Glu86 in F86D and F86E, respectively, upon retinal isomerization. In BR$_K$, there is no structural change for the corresponding residue, Asp96. We previously showed that more extensive protein structural changes occur during the formation of K in *p*pR than in BR (*22*). Greater structural changes are observed at position 105 in *p*pR than at the corresponding position 115 in BR, which is located ∼7 Å from the retinal chromophore (*39*). However, it is likely that structural changes do not reach position 86, which is ∼12 Å from the retinal at the K state (Figure 1a).

Infrared Spectral Changes of the F86D and F86E Mutants of ppR Measured at 250 K. Figure 3 shows the *p*pR$_M$ minus *p*pR infrared difference spectra of F86D (a) and F86E (b) measured at 250 K and pH 7. These spectra are compared with the previously reported spectrum for the wild-type protein (···) (*24*). The ethylenic C═C stretching mode of the unphotolyzed state appears as a negative peak at 1545 cm^{-1} for both F86D (a) and F86E (b), and is identical to that of the wild type (*24*). Like the *p*pR$_K$ minus *p*pR spectra (Figure 2), almost identical difference spectra were obtained for F86D and F86E except for the protonated carboxylic C═O stretching region, suggesting similar protein structural changes on formation of *p*pR$_M$ among F86D, F86E, and the wild type.

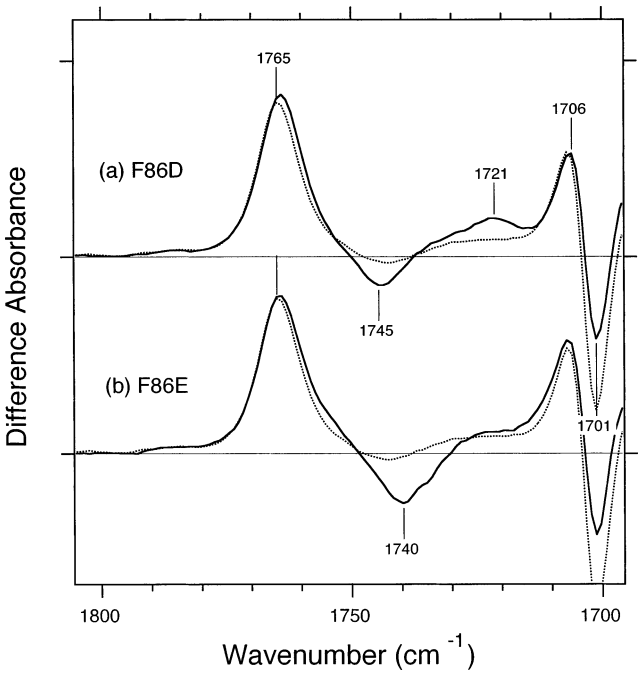

FIGURE 4: *p*pR$_M$ minus *p*pR IR difference spectra of F86D (a) and F86E (b) in the 1805−1695 cm^{-1} region. Spectra are measured at 250 K and pH 7. Difference IR spectra of the wild type (*24*) are reproduced as dotted lines for comparison.

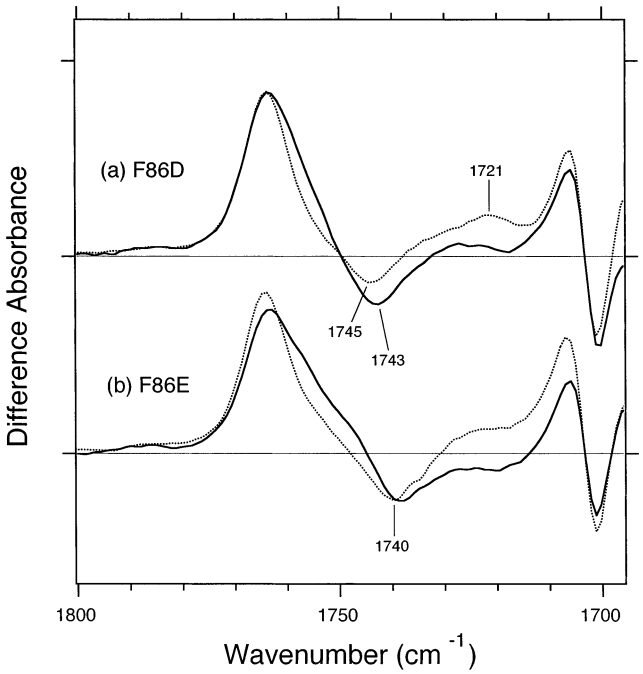

FIGURE 5: Difference IR spectra of F86D (a) and F86E (b) at 270 K and pH 9 in the 1800−1695 cm^{-1} region. *p*pR$_M$ minus *p*pR IR difference spectra of F86D [a (···)] and F86E [b (···)] at 250 K and pH 7 are reproduced from traces a and b of Figure 4 (—), respectively.

Certain spectral differences were observed in the 1800−1700 cm^{-1} region which monitors the C═O stretching vibrations of protonated carboxylates (Figure 4). The positive peak of the wild type (···) at 1765 cm^{-1} originates from the C═O stretch of Asp75, as a consequence of the proton transfer from the Schiff base to Asp75 upon formation of *p*pR$_M$ (*24*). The frequency is identical in F86D (a) and F86E (b). The environment of Asp75 is highly hydrophobic in F86D, F86E, and the wild type, as well as the environment for Asp85 in BR (*24*). In addition, the bands at 1706 (+) and 1701 (−) cm^{-1} are due to the C═O stretch of Asn105 (*24*), and they are not influenced by the mutation at position 86.

Characteristic spectral features of the Phe86 mutants are the appearance of a negative band at 1745 and 1740 cm^{-1} in F86D (a) and F86E (b), respectively. In F86D, a positive peak also appeared at 1721 cm^{-1} (a). In contrast, no clear positive peak was observed in F86E (b). These new bands were shifted to 1741 (−)/1714 (+) and 1736 (−) cm^{-1} for F86D and F86E, respectively, in D_2O (data not shown). Thus, it is likely that the new bands originate from the carboxylic C═O stretches of the protonated Asp86 or Glu86. This observation implies that the pK_a of Asp86 and Glu86 is higher than 7, which is consistent with the highly hydrophobic environment around position 86 in the crystal structure of *p*pR (Figure 1a).

The BR$_M$ minus BR spectrum exhibits the 1742 (−)/1736 (+) cm^{-1} bands because of the alteration of the Asp96 hydrogen bonds (*40*). Thus, similar environmental changes occur at Asp86 in the F86D mutant of *p*pR upon formation of M. Having a lower frequency (1721 cm^{-1}) (Figure 4a) than that of Asp96 in BR (1736 cm^{-1}) implies a stronger hydrogen bond of the C═O group in F86D. No positive peak in the *p*pR$_M$ minus *p*pR spectra of F86E (Figure 4b) suggests that Glu86 is deprotonated in the M state. The positive peak at 1395 cm^{-1} (Figure 3b) may originate from the stretching vibration of the deprotonated Glu86. The proton from Glu86 may be transferred to an internal proton acceptor, or released to the aqueous phase. The Schiff base cannot be the acceptor, because the infrared spectrum of F86E (Figure 3b) exhibits fingerprint vibrations (1300−1100 cm^{-1}) identical to those of the wild type. This fact strongly suggests that the intermediate of F86E possesses a deprotonated retinal Schiff base.

Infrared Spectral Changes of the F86D and F86E Mutants of ppR Measured at 270 K. The infrared spectra of F86D and F86E at 250 K clearly showed the structural changes of Asp86 and Glu86 (Figure 4), respectively. Since proton pump activity is enhanced in these mutants, Asp86 and Glu86 are probably involved in the proton transport, and the observed structural changes are correlated with such function. However, there was no evidence of proton transfer from Asp86 or Glu86 to the Schiff base at 250 K, even though Glu86 appears to be deprotonated in the M state of F86E. Therefore, we next measured the spectra at higher temperatures, where further protein structural changes should take place. We prepared an alkaline film in this study, because the neutral film sample produces both M and O intermediates at >250 K that makes the analysis complicated. In contrast, at pH 9, only the M state is formed in a wide temperature range (250−290 K), where neither the N nor the O state was formed (*24*).

Figure 5 compares the spectrum measured at 270 K for the hydrated film at pH 9 with that in Figure 4 (250 K and pH 7). The negative peaks at 1743 (a) and 1740 cm^{-1} (b) were present at pH 9 in F86D and F86E, respectively, indicating the protonation of Asp86 and Glu86 in the unphotolyzed state, respectively. The pK_a values of the carboxylates are thereby >9. In F86D, the positive peak at 1721 cm^{-1} in the *p*pR$_M$ minus *p*pR spectrum at 250 K [Figure

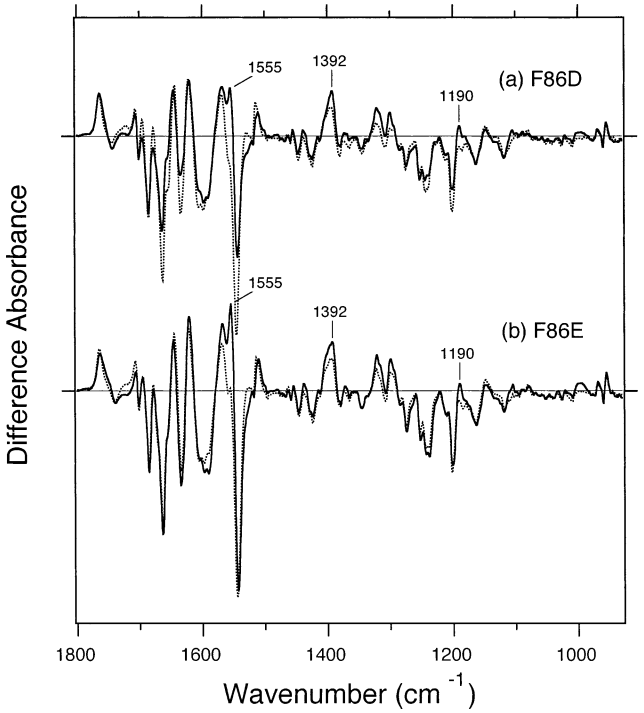

FIGURE 6: Difference IR spectra of F86D (a) and F86E (b) at 270 K and pH 9 in the 1800−920 cm^{-1} region. *p*R_M minus *p*R IR difference spectra of F86D [a (···)] and F86E [b (···)] at 250 K and pH 7 are reproduced from traces a and b of Figure 3 (—), respectively.

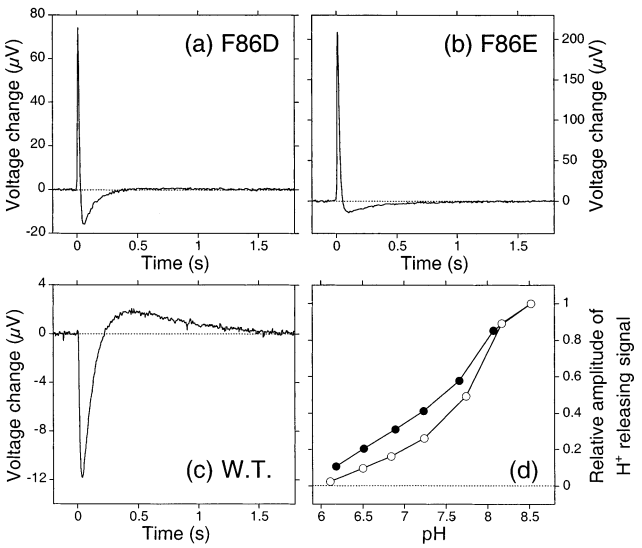

FIGURE 7: (a−c) Photoelectrochemical responses of F86D (a), F86E (b), and the wild type (c) at 293 K and pH 7.0. A positive signal is due to a decrease in the local pH, i.e., proton release from *p*pR, and a negative signal is caused by proton uptake. The electrolyte solution contained 0.13 M Na_2SO_4 and a mixture of six buffers (see Materials and Methods). (d) Relative amplitudes of the first proton releasing (positive) signals of F86D (○) and F86E (●) at varying pHs. Each maximum value is adjusted to 1.

5a (···)] disappeared at 270 K (—), presumably because of deprotonation of Asp86. Spectral differences were also observed for F86E, where the absorbance at 1730−1710 cm^{-1} decreases at 270 K (Figure 5b). We inferred that Glu86 is already deprotonated at 250 K from the spectral comparison between F86E and the wild type (Figure 4). Nevertheless, Figure 5b suggests the presence of the positive signal at 1730−1710 cm^{-1}; thus, Glu86 is partially, not fully, deprotonated at 250 K, and deprotonation of Glu86 is complete at 270 K.

Asp86 or Glu86 is deprotonated at 270 K for the hydrated film of F86D or F86E, respectively. Then, the next question is the location to which the proton is transferred. Figure 6 shows a wider frequency region (1800−920 cm^{-1}) than Figure 5. This figure clearly exhibits the appearance of the positive peak at 1190 cm^{-1} in both F86D (a) and F86E (b). This band is characteristic of an N-like chromophore, i.e., protonated 13-*cis* form (*40*). In addition, the appearance of the positive peak at 1555 cm^{-1} in both F86D (a) and F86E (b) is also characteristic of an N-like state. Since protonation of the chromophore is accompanied by deprotonation of carboxylates at position 86, it is likely that the proton transfer takes place from Asp86 or Glu86 to the Schiff base. Part of the strong positive band at 1392 cm^{-1} may originate from the stretching vibration of the deprotonated Asp86 (a) or Glu86 (b).

The intermediate of the Phe86 mutants of *p*pR at 270 K possesses deprotonated carboxylates at position 86 and a protonated 13-*cis* chromophore, which are characteristic of the N state of BR. An N-specific protein structure can be described in the BR_N minus BR spectrum by the highly dichroic strong amide I vibrations at 1671 (−), 1663 (+), and 1649 (+) cm^{-1} (*41*). Interestingly, the amide I vibrations of the difference spectra at 270 K (solid lines in Figure 6) were almost identical with those of the *p*pR_M minus *p*pR spectrum at 250 K (dotted lines in Figure 6). This fact implies that the intermediate of the *p*pR mutants at 270 K possesses an M-like protein structure, not an N-like one. In other words, proton transfer from Asp86 or Glu86 may takes place without large protein structural changes.

It is also noted that the intensity of the positive 1190 cm^{-1} band is smaller than that of the BR_N minus BR spectrum (*41*), suggesting that all protons of carboxylates at position 86 may not necessarily be transferred to the Schiff base. In fact, deprotonation of Glu86 at 250 K (Figure 4b) is not accompanied by protonation of the Schiff base (Figure 3b). Therefore, the proton of Glu86 needs to be transferred to another internal acceptor or released to the aqueous phase. To examine the latter possibility, we next studied photoelectrochemical responses of the Phe86 mutants.

Photoelectrochemical Responses of the F86D and F86E Mutants of ppR. We measured photoelectrochemical signals of F86D and F86E by using the SnO_2 electrode to investigate proton uptake and release during their photocycles. Figure 7 shows the flash-induced photoelectrochemical responses of F86D (a), F86E (b), and the wild type (c) measured at pH 7. The SnO_2 electrode is highly sensitive to a pH change at the electrode surface (*34*−*36*, *42*). A time-differentiated positive signal is due to a decrease in the local pH, i.e., proton release from *p*pR, and a negative signal is caused by proton uptake. A previous study of wild-type *p*pR solubilized in DM showed that proton uptake preceded proton release during the photocycle, and that uptake and release coincide with the formation and decay of ppR_O, respectively (*37*). Essentially the same result was obtained for wild-type *p*pR reconstituted into PC liposomes (Figure 7c), where NaCl in an electrolyte solution was replaced with Na_2SO_4 in the present measurement. In Figure 7c, after light excitation, a negative signal followed by a slow positive signal was

observed, indicating the proton uptake and following release during the photocycle of *p*pR. The crossover point at zero represents the time to reach the peak of the pH change. This value for the wild type (~200 ms, Figure 7c) was close to the time at which $p$ppR$_O$ accumulates mostly during the photocycle (*1*, *6*), showing proton uptake and release coincide with the formation and decay of $p$ppR$_O$, respectively. A previous study of pR from *Halobacterium salinarum* suggested that the signal of proton uptake and release predominantly originates from the groups at the extracellular side (*43*).

Panels a and b of Figure 7 show the photoelectrochemical responses of F86D and F86E, respectively. In contrast to the wild type, for F86D and F86E a sharp positive signal appears, followed by a relatively slow negative signal. These results suggest that proton release precedes proton uptake during the photocycle of the Phe86 mutants. A fast increase in the positive signal implies that proton release takes place before the formation of the O state. Therefore, proton release presumably occurs in the M state. Together with the FTIR data, we concluded that the proton release signals in F86D and F86E originate from deprotonation of Asp86 and Glu86, respectively. There is a third positive component in the 0.5−1.5 s region of F86D (Figure 7a), which coincides with that of the wild type (Figure 7c). Replacement of Phe86 with Asp at the cytoplasmic side is not likely to change the proton uptake and release at the extracellular side. We infer that the lack of a signal like that of the wild type in F86E (Figure 7b) is caused by (i) the slower recovery of the negative signal in F86E (up to 1 s) than in F86D and (ii) the greater amplitude of the signal in F86E than in F86D. These factors would mask the signal like that of the wild type present in F86E.

The signal amplitudes of our photoelectrochemical measurements are not necessarily quantitative, because adsorption of the reconstituted *p*ppR samples was not perfectly controlled. Since the release signal appears to depend on pH, we next tested the pH dependence of the photoelectrochemical responses of F86D and F86E. Figure 7d shows the relative amplitudes of the first proton releasing signals in F86D (○) and F86E (●) at varying pHs. Under acidic conditions (pH <6), proton uptake precedes release also in the case of Phe86 mutants (data not shown). Fast proton release (Figure 7a,b) was detected at pH >6; the amplitudes seem to be saturated at pH 8.5−9.0. Kinetic profiles were similar between pH 7 and 9, while amplitudes were stronger at alkaline pH (not shown). Figure 7d suggests that the pK_a of Asp86 and Glu86 in the M state is ~7.5, and slightly higher in Asp86. The stronger proton affinity at position 86 in the M state of F86D is consistent with the infrared spectra in Figure 4, where F86D only exhibits a positive band at 1721 cm^{-1}.

DISCUSSION

In this paper, we analyzed proton transfer reactions during the photocycles of the F86D and F86E mutants of *p*pR by using FTIR spectroscopy and photoelectrochemical methods. The $p$ppR$_K$ minus *p*pR spectra of the Phe86 mutants were identical to that of the wild type (Figure 2). We concluded that the protein structural changes in $p$ppR$_K$ that are more extended than those in BR$_K$ (*22*) do not involve change at position 86, which is ~12 Å from the retinal chromophore (Figure 1a).

FTIR spectroscopy revealed the unique environmental changes around position 86 in the M intermediate, though the $p$ppR$_M$ minus *p*pR spectra of the Phe86 mutants were similar to that of the wild type (Figure 3). Asp86 or Glu86 is protonated in F86D or F86E, respectively, and their pK_a values > 9. They drop to release a proton in late intermediates. This feature is also noted in BR, where the direction of the proton from Asp96 is toward the Schiff base. In contrast, protons are released from Asp86 or Glu86 to the cytoplasmic aqueous phase in the Phe86 mutants of *p*pR, as revealed by the photoelectrochemical measurements (Figure 7). The pK_a values in the M-like states are ~7.5, and slightly higher in Asp86 (Figure 7d). A longer side chain in F86E might destabilize the protonation state of Glu86 in the M-like intermediate.

Our FTIR data indicated protonation changes in both carboxylates at position 86 and the Schiff base. Therefore, it is evident that there is a transient proton channel in the cytoplasmic region of the mutant *p*pR, which is presumably used by the proton pump (*26*). An interesting observation is that a proton is released to the aqueous phase even though there is a proton channel between Asp86 or Glu86 and the Schiff base. A similar observation, i.e., proton release from Asp96, has been reported for some BR mutants, such as D85N (*44*, *45*) and the blue form of D212N (*46*). In these cases, however, the proton acceptor of Asp96, the Schiff base, is protonated during the photocycle so that Asp96 has to release a proton to the cytoplasmic aqueous phase when its pK_a is lowered. Our finding with the mutant *p*pR is unique in this sense; a proton is released despite the presence of the deprotonated Schiff base in $p$ppR$_M$. This suggests that there is a mechanism that prevents an internal proton transfer from Asp86 or Glu86 to the Schiff base in the mutant *p*pR. In other words, BR has a specific mechanism that conducts a proton uniquely from Asp96 to the Schiff base (*47*−*49*). Even when the pK_a of Asp96 is first lowered in BR, Asp96 is likely to be inaccessible to the bulk in the M-to-N transition. This makes the direction of a proton from Asp96 to the Schiff base. Then, Asp96 is open to the bulk for proton uptake. This mechanism seems to be lacking in *p*pR. In *p*pR, the open structure at the cytoplasmic side appears to be formed at once so that a proton can be conducted from Asp86 or Glu86 in either direction, the Schiff base or the bulk.

Proton conduction from Asp86 or Glu86 to the Schiff base seems to be less favorable in the mutant *p*pR than in BR. Interestingly, protein structures of the unphotolyzed states of *p*pR and BR are similar (Figure 1). Therefore, such a difference should be explained in terms of protein structural changes. In this regard, the appearance of the N-like protein structure may be an important factor. BR$_N$ possesses the 13-*cis* chromophore with a protonated Schiff base, deprotonated Asp96, and largely changed protein structure. Protonation of the Schiff base is not a prerequisite for the formation of N-like structure in BR. When Asp96 is replaced with Asn, the M state is highly stabilized at alkaline pH. Previous FTIR spectroscopy of the D96N protein of BR revealed the appearance of the M$_N$ state after M, where the chromophore is M-like (deprotonated) but the protein structure is N-like (largely changed) (*50*). We recently found that *p*pR does not have such an N-like protein structure even at alkaline pH (*24*). Our study clearly showed that there are no N-like protein backbone structures, even though the N-like state

appeared in terms of the 13-*cis* chromophore with protonated Schiff base and deprotonated carboxylates at position 86 (Figure 6). Thus, the lack of the N-like protein structure may be correlated with the unique property of *p*pR (the mutant *p*pR).

It is noted that an opening of the F helix is reported for *p*pR as well as for BR in a spin-labeling experiment (*51*, *52*), which is consistent with the observation that the proton conducting channel is transiently formed at the cytoplasmic side. Nevertheless, protein structural changes leading to F helix opening might be different between *p*pR and BR. In BR, Asp96 forms a hydrogen bond with Thr46 in the B helix, while the corresponding amino acids of *p*pR are phenylalanine and valine at positions 86 and 40, respectively. We previously reported that the F86D/L40T mutant *p*pR (*28*, *53*) has much shorter photocycle kinetics than F86D and the wild type, being similar to those of BR. Therefore, it is interesting to examine the protein structural changes and proton transfer reactions in F86D/L40T, which is our next focus.

ACKNOWLEDGMENT

We thank Y. Sudo and Dr. K. Shimono for valuable discussion.

REFERENCES

1. Chizhov, I., Schmies, G., Seidel, R., Sydor, J. R., Lüttenberg, B., and Engelhard, M. (1998) *Biophys. J. 75*, 999−1009.
2. Engelhard, M., Scharf, B., and Siebert, F. (1996) *FEBS Lett. 395*, 195−198.
3. Hirayama, J., Imamoto, Y., Shichida, Y., Kamo, N., Tomioka, H., and Yoshizawa, T. (1992) *Biochemistry 31*, 2093−2098.
4. Hirayama, J., Imamoto, Y., Shichida, Y., Yoshizawa, T., Asato, A. E., Liu, R. S., and Kamo, N. (1994) *Photochem. Photobiol. 60*, 388−393.
5. Hirayama, J., Kamo, N., Imamoto, Y., Shichida, Y., and Yoshizawa, T. (1995) *FEBS Lett. 364*, 168−170.
6. Miyazaki, M., Hirayama, J., Hayakawa, M., and Kamo, N. (1992) *Biochim. Biophys. Acta 1140*, 22−29.
7. Scharf, B., Pevec, B., Hess, B., and Engelhard, M. (1992) *Eur. J. Biochem. 206*, 359−366.
8. Seidel, R., Scharf, B., Gautel, M., Kleine, K., Oesterhelt, D., and Engelhard, M. (1995) *Proc. Natl. Acad. Sci. U.S.A. 92*, 3036−3040.
9. Oesterhelt, D., and Stoeckenius, W. (1971) *Nat. New Biol. 233*, 149−152.
10. Lanyi, J. K. (2000) *Biochim. Biophys. Acta 1460*, 1−3.
11. Matsuno-Yagi, A., and Mukohata, Y. (1977) *Biochem. Biophys. Res. Commun. 78*, 237−243.
12. Lanyi, J. K. (1990) *Physiol. Rev. 70*, 319−330.
13. Varo, G. (2000) *Biochim. Biophys. Acta 1460*, 220−229.
14. Bogomolni, R. A., and Spudich, J. L. (1982) *Proc. Natl. Acad. Sci. U.S.A. 79*, 6250−6254.
15. Hoff, W. D., Jung, K. H., and Spudich, J. L. (1997) *Annu. Rev. Biophys. Biomol. Struct. 26*, 223−258.
16. Spudich, J. L., Yang, C. S., Jung, K. H., and Spudich, E. N. (2000) *Annu. Rev. Cell Dev. Biol. 16*, 365−392.
17. Shimono, K., Iwamoto, M., Sumi, M., and Kamo, N. (1997) *FEBS Lett. 420*, 54−56.
18. Kamo, N., Shimono, K., Iwamoto, M., and Sudo, Y. (2001) *Biochemistry (Moscow) 66*, 1277−1282.
19. Luecke, H., Schobert, B., Lanyi, J. K., Spudich, E. N., and Spudich, J. L. (2001) *Science 293*, 1499−1503.
20. Royant, A., Nollert, P., Edman, K., Neutze, R., Landau, E. M., Pebay-Peyroula, E., and Navarro, J. (2001) *Proc. Natl. Acad. Sci. U.S.A. 98*, 10131−10136.
21. Gordeliy, V. I., Labahn, J., Moukhametzianov, R., Efremov, R., Granzin, J., Schlesinger, R., Büldt, G., Savopol, T., Scheidig, A. J., Klare, J. P., and Engelhard, M. (2002) *Nature 419*, 484−487.
22. Kandori, H., Shimono, K., Sudo, Y., Iwamoto, M., Shichida, Y., and Kamo, N. (2001) *Biochemistry 40*, 9238−9246.
23. Imamoto, Y., Shichida, Y., Hirayama, J., Tomioka, H., Kamo, N., and Yoshizawa, T. (1992) *Photochem. Photobiol. 56*, 1129−1134.
24. Furutani, Y., Iwamoto, M., Shimono, K., Kamo, N., and Kandori, H. (2002) *Biophys. J. 83*, 3482−3489.
25. Schmies, G., Luttenberg, B., Chizhov, I., Engelhard, M., Becker, A., and Bamberg, E. (2000) *Biophys. J. 78*, 967−976.
26. Schmies, G., Engelhard, M., Wood, P. G., Nagel, G., and Bamberg, E. (2001) *Proc. Natl. Acad. Sci. U.S.A. 98*, 1555−1559.
27. Sudo, Y., Iwamoto, M., Shimono, K., Sumi, M., and Kamo, N. (2001) *Biophys. J. 80*, 916−922.
28. Iwamoto, M., Shimono, K., Sumi, M., and Kamo, N. (1999) *Biophys. Chem. 79*, 187−192.
29. Miyasaka, T., Koyama, K., and Itoh, I. (1992) *Science 255*, 342−344.
30. Miyasaka, T., Koyama, K., and Itoh, I. (1992) *Thin Solid Films 210/211*, 146.
31. Koyama, K., Yamaguchi, N., and Miyasaka, T. (1994) *Science 265*, 762−765.
32. Koyama, K. (1997) *Photochem. Photobiol. 66*, 784−787.
33. Koyama, K., Miyasaka, T., Needleman, R., and Lany, J. K. (1998) *Photochem. Photobiol. 68*, 400−406.
34. Robertson, B., and Lukashev, E. P. (1995) *Biophys. J. 68*, 1507−1517.
35. Wang, J. P., Yoo, S. K., Song, L., and El-Sayed, M. A. (1997) *J. Phys. Chem. B 101*, 3420−3423.
36. Wang, J. P., Song, L., Yoo, S. K., and El-Sayed, M. A. (1997) *J. Phys. Chem. B 101*, 10599−10604.
37. Iwamoto, M., Shimono, K., Sumi, M., Koyama, K., and Kamo, N. (1999) *J. Phys. Chem. B 103*, 10311−10315.
38. Kandori, H., Furutani, Y., Shimono, K., Shichida, Y., and Kamo, N. (2001) *Biochemistry 40*, 15693−15698.
39. Kandori, H., Shimono, K., Shichida, Y., and Kamo, N. (2002) *Biochemistry 41*, 4554−4559.
40. Maeda, A. (1995) *Isr. J. Chem. 35*, 387−400.
41. Kandori, H. (1998) *J. Am. Chem. Soc. 120*, 4546−4547.
42. Saga, Y., Watanabe, T., Koyama, K., and Miyasaka, T. (1999) *J. Phys. Chem. B 103*, 234−238.
43. Sasaki, J., and Spudich, J. L. (1999) *Biophys. J. 77*, 2145−2152.
44. Otto, H., Marti, T., Holz, M., Mogi, T., Stern, L. J., Engel, F., Khorana, H. G., and Heyn, M. P. (1990) *Proc. Natl. Acad. Sci. U.S.A. 87*, 1018−1022.
45. Kataoka, M., Kamikubo, H., Tokunaga, F., Brown, L. S., Yamazaki, Y., Maeda, A., Sheves, M., Needleman, R., and Lanyi, J. K. (1994) *J. Mol. Biol. 243*, 621−638.
46. Cao, Y., Brown, L. S., Needleman, R., and Lanyi, J. K. (1993) *Biochemistry 32*, 10239−10248.
47. Balashov, S. P. (2000) *Biochim. Biophys. Acta 1460*, 75−94.
48. Subramaniam, S., and Henderson, R. (2000) *Nature 406*, 653−657.
49. Dioumaev, A. K., Brown, L. S., Needleman, R., and Lanyi, J. K. (2001) *Biochemistry 40*, 11308−11317.
50. Sasaki, J., Shichida, Y., Lanyi, J. K., and Maeda, A. (1992) *J. Biol. Chem. 267*, 20782−20786.
51. Wegener, A. A., Chizhov, I., Engelhard, M., and Steinhoff, H. J. (2000) *J. Mol. Biol. 301*, 881−891.
52. Wegener, A. A., Klare, J. P., Engelhard, M., and Steinhoff, H. J. (2001) *EMBO J. 20*, 5312−5319.
53. Klare, J. P., Schmies, G., Chizhov, I., Shimono, K., Kamo, N., and Engelhard, M. (2002) *Biophys. J. 82*, 2156−2164.
54. Luecke, H., Schobert, B., Richter, H.-T., Cartailler, J. P., and Lanyi, J. K. (1999) *J. Mol. Biol. 291*, 899−911.

BI0270283